MPPT Full Bridge Converter Using Fuzzy Type-2 on DC Nano Grid System

Annas Budi Prastyawan
Department of Electrical Engineering
Politeknik Elektronika Negeri Surabaya
Surabaya, Indonesia
annasbudip98@gmail.com

Mohammad Zaenal Efendi
Department of Electrical Engineering
Politeknik Elektronika Negeri Surabaya
Surabaya, Indonesia
zen@pens.ac.id

Farid Dwi Murdianto
Department of Electrical Engineering
Politeknik Elektronika Negeri Surabaya
Surabaya, Indonesia
farid@pens.ac.id

***Abstract*—Renewable energy applications using Photovoltaics (PV) is developed as a conversion of solar energy into electrical energy. PV produce output power according to irradiation and temperature conditions. PV has a Maximum Power Point or MPP based on P-V characteristic curve. In certain conditions, PV has an unstable output power so that the accuracy of the power generated is not maximum. MPPT method with conventional control is not optimal to resolves power inaccuracies in the system. When the system has a circuit problem, conventional power converter will damage overall to maximize and accurate PV output power. Maximum Power Point method will look for MPP. MPPT uses Fuzzy Type-2 Algorithm in the converter which can reliably overcome inaccuracy and tracking speed of the PV power. Using Full Bridge Converter topology, the circuit security system uses a high frequency isolated transformer. Implemented on MATLAB/Simulink software, simulation results in Model 1 show that the average power accuracy with Fuzzy Type-2 is 91.40% compared to Fuzzy Type-1 with an average power accuracy of 80.64%. In Model 2, Fuzzy Type-2 is 87.63% compared to Fuzzy Type-1 of 77.93%. MPPT method using fuzzy type-2 is better than using fuzzy type-1 in terms of power accuracy.**

Keywords—full bridge converter, fuzzy type-2, MATLAB/Simulink, maximum power point tracking, photovoltaic.

I. INTRODUCTION

Environmental pollution and rising fuel prices are unfavorable factors for power plants that use fossil fuels. Renewable energy becomes alternative energy which is expected to change the distribution pattern and current electricity generation system. There are various types of renewable energy that are used to produce electrical energy, one of which is solar energy. It was explained [1] that the advantages of alternative energy with solar panels do not require a fossil fuel source, do not cause environmental pollution, require less maintenance time, and do not make noise compared to other renewable energies.

As it is well known that renewable energy such as solar panels has non-linear characteristics and produces an output power that varies depending on environmental conditions such as irradiation and temperature. Therefore, the best efficiency from using solar panels as a source of electrical energy with a power converter system needs to be operated at Maximum Power Point (MPP). Several algorithms used as methods have been proposed to maximize the output power of solar panels, such as Perturb and Observe [2], Hill Climbing, Artificial Network [3], and Fuzzy Logic [4]. Based on the features of the MPPT categorized by the number of control variables, control strategies made, sequences, and manufacturing cost [5].

The operation of the system which is designed to be operated on MPP uses the Fuzzy Type-2 Algorithm control. The control output functions as a regulator of the power converter duty cycle parameter values to achieve maximum tracking of the Solar Panel output power according to MPP. Fuzzy Type-2 Algorithm is a development of Fuzzy logic control. The conditions of resilience, dynamic, and uncertainty from simple to complex are suitable for use in fuzzy control, for example for solar panels. Based on [6] in terms of Adaptive and renewal, it is the difference in control of Fuzzy Type-2 and Fuzzy Type-1. The use of control to reduce transient values and fluctuations around the maximum power is the advantage of Fuzzy Type-2. The DC-DC converter system implemented for sensitive loads with dynamic response will have an impact on the use of Fuzzy Type-2 control compared to Fuzzy Type-1. The membership function in the two different controls is one of the contributing factors [7].

DC-DC converters with Full Bridge Converter topology, are used in systems designed for solar panels. The converter is implemented as a DC voltage converter with a voltage booster type, and to adjust the value of the duty cycle so that the maximum power point (MPP) is obtained at each irradiation and temperature. The implementation of medium to high power and the ratio of the increase in the voltage ratio are characteristics that can be applied to the Full Bridge Converter [8].The converter circuit in the system is divided into two stages in converting the voltage value, namely the high-frequency switching process in a full bridge circuit giving a square AC wave to a high frequency isolated transformer on the primary side, and on the secondary side it will be rectified into a DC wave with a full bridge rectifier [9]. The use of an LC filter to reduce voltage losses before connecting to the load.

Of all the references that have been described, the research discussed in this paper includes the design of the MPPT method which is selected using the Fuzzy Type-2 Algorithm, with the Full Bridge Converter topology as a power conversion tool. This paper also discusses the simulation and analysis of changes in irradiation and temperature on the tracking power to its maximum point using a comparison of the MPPT Fuzzy Type-1 and Fuzzy type-2 methods.

II. METHODS

The methods used in this research will be explained as follows.

A. Photovoltaic Modelling and Characteristic System

Cell in the solar panel based on [10] is a representation of a diode that has a cell current value (I_C) with reverse-biased current conditions and contains a small value. If the solar panel is at no load, the current value of the diode will be $I_D = I_C$. In the application of the load current (I_L) is related to the diode current (I_D) shown in equation 1.

$$I_{Load} = I_{Cell} - i_{Diode} = I_{Cell} - I_S\left(e^{V_{diode}/\eta V_T} - 1\right) \quad (1)$$

The solar panel generates a short circuit current (I_{SC}) with the value of $I_{SC} = I_C$ when the output side of the solar panel is short circuited. The value of the open circuit voltage (V_{OC}) can be determined by equation 2.

$$V_{OC} = V_{diode} = V_T \ln\left(\frac{I_{Cell}}{I_S} + 1\right) \quad (2)$$

The Solar Panel (P_L) output power can be determined for $V_L = V_D$ from equation 3.

$$P_{Load} = V_{Load}I_{Load} = V_{Load}\left[I_{Cell} - V_{Load}I_S\left(e^{V_{Load}/\eta V_T} - 1\right)\right] \quad (3)$$

Using the first derivative of the output power $P_L = 0$, we can find the load voltage (V_{MP}) obtained at the maximum power condition (P_{MP}) by equation 4.

$$\frac{\delta P_{Load}}{\delta V_{Load}} = (I_{Cell} + I_S) - \left(1 + \frac{V_{Load}}{V_T}\right) I_S e^{V_{Load}/\eta V_T} = 0 \quad (4)$$

At maximum power conditions, voltage (V_{MP}) for $\frac{\delta P_{Load}}{\delta V_{Load}} = 0$ so that equation 5.

$$\left(1 + \frac{V_{MP}}{V_T}\right) e^{V_{MP}/\eta V_T} = \left(1 + \frac{I_{Cell}}{I_S}\right) \quad (5)$$

The maximum output power (P_{max}) is obtained from the operating conditions when $V_L = V_{MP}$, by substituting the maximum voltage (V_{MP}) in equation 3 and equation 6 is obtained.

$$P_{Max} = V_{MP}\left[I_{Cell} - V_{MP}I_S\left(e^{V_{MP}/\eta V_T} - 1\right)\right] \quad (6)$$

A solar panel has a loss value during practical implementation conditions, namely on the external cable and trace collector, so that the value of series resistance (R_S) and parallel resistance (R_P) is obtained. Due to losses, the load current value according to equation 1 will be reduced as shown in Equation 7.

$$I_{Load} = I_{Cell} - i_{Diode} = I_{Cell} - I_S\left(e^{V_{diode}/\eta V_T} - 1\right) - \frac{V_{Diode}}{R_P} \quad (7)$$

In addition, just like the load current (I_L), the value of the load voltage (V_L) will experience losses so that it is reduced according to equation 8.

$$V_{Load} = V_{Diode} - R_S I_{Load} = V_{Diode} - R_S\left[I_{Cell} - I_S\left(e^{V_{diode}/\eta V_T} - 1\right) - \frac{V_{Diode}}{R_P}\right] \quad (8)$$

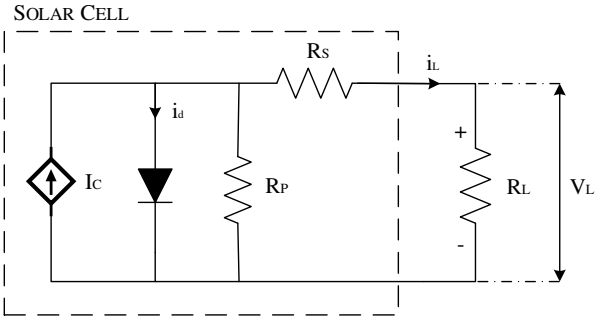

Fig. 1. Photovoltaic equivalent circuit.

The model of the solar panel in practical implementation conditions is shown in Figure 1, with the solar panel connected to the load.

TABLE I. PHOTOVOLTAIC DATASHEET SYSTEM

Parameter	Value
P_{max}	100 W
V_{mp}	17.8 V
I_{mp}	5.62 A
V_{oc}	21.8 V
I_{sc}	6.05 A
Dimension	1125 x 670 x 30 mm
Test Condition	1000 W/m2, 25°C

In Table 1, the parameter values on the solar panel are shown according to the datasheet used in the system as a source of electrical energy. In accordance with the system design, the solar panels used are 2 ST-Solar Polycrystalline 100 WP solar modules arranged in series to produce a solar panel output power of 200 watts.

B. Full Bridge Converter

The topology of full bridge converter is shown on Figure 2 as a system implementation using a magnetic core and semi-conductor switching components so that it is more efficient to use in medium to high power applications ranging from hundreds to thousands of watts. The structure of the converter circuit consists of H-bridge switching, high frequency isolation transformer, full bridge rectifier, and an LC filter before going to the load.

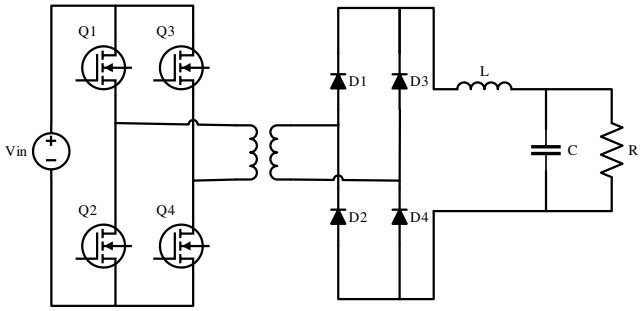

Fig. 2. Full Bridge converter circuit.

The current flow from the input to output power conversion by using high-frequency semiconductor

switching components, through the process of the four conditions described in Figure 3 and Figure 4.

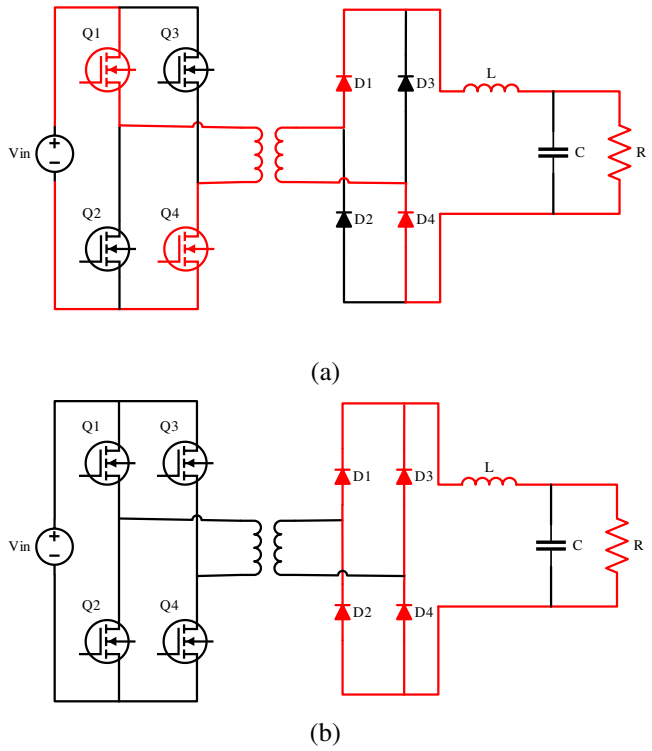

Fig. 3. The current flow in the converter during the switching process in components Q1 and Q4 (a) when condition 1 (b) when condition 2.

Figure 3a shows that when the converter is in condition 1, the current will flow through Q1 and Q4 because the two switching components are closed or ON, while Q2 and Q3 are not energized because they are open or OFF. The positive primary side voltage will be forwarded to the secondary side of the transformer and diodes D1 and D4 flow current to the filter circuit and converter output.

In condition 1, the time period 0 < t < dT, the two switching components Q1 and Q4 close or ON simultaneously, and the secondary side has a voltage that is valued in accordance with equation 9.

$$V_{sec} = \frac{N_s}{N_p} V_{in} \tag{9}$$

The value of the output inductor voltage (V_L) is equation 10.

$$V_L = \frac{N_s}{N_p} V_{in} - V_{out} \tag{10}$$

The value of the inductor output current (I_L) will increase linearly according to equation 11.

$$\frac{di_L}{d_t} = \frac{V_L}{L} = \frac{1}{L}\left[\frac{N_s}{N_p} V_{in} - V_{out}\right] \tag{11}$$

The termination of condition 1 with the value of the peak inductor current ($I_{L(peak)}$) when t = dT, is shown in equation 12.

$$I_{L(peak)} = I_L(0) + \frac{1}{L}\left[\frac{N_s}{N_p} V_{in} - V_{out}\right] \tag{12}$$

Figure 3b shows when the converter is in condition 2, the first deadtime process occurs with the four switching components in the open or OFF condition so that the output current flows to the four diodes. In condition 2, the time period dT < t ≤ T / 2, the drop rate in inductor current (I_L) is according to equation 13.

$$\frac{di_L}{d_t} = \frac{V_{out}}{L}; \text{towards } 0 < t < (0.5 - d)T \tag{13}$$

The value of the inductor output current at 0 seconds (IL(0)) is obtained from equation 14.

$$I_L(0) = i_L[t = (0.5 - d)T] = I_{L(peak)} - V_{out}(0.5 - d)\frac{T}{L} \tag{14}$$

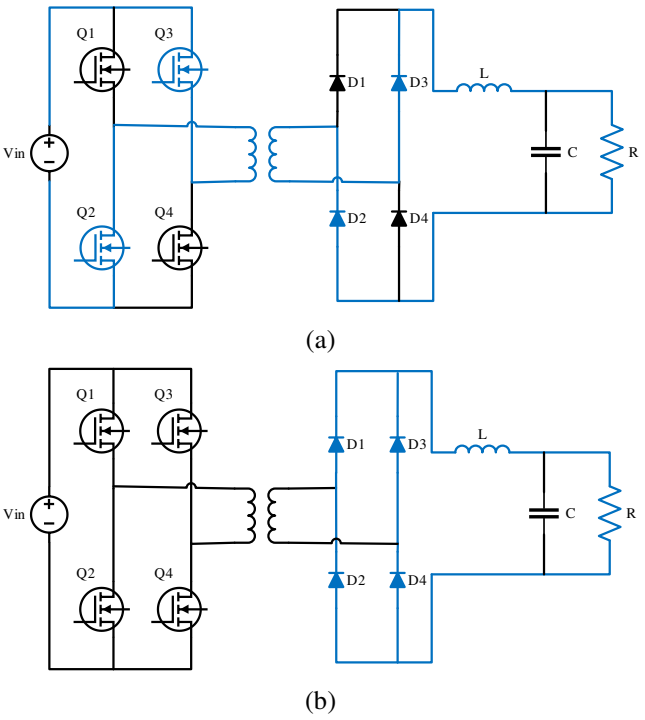

Fig. 4. The current flow in the converter during the switching process in components Q2 and Q3 (a) when condition 3 (b) when condition.4

Figure 4a shows when the converter is in condition 3, the same as the operation that occurs in condition 1. Current flows through Q2 and Q3 because the two switching components are closed or ON, while Q1 and Q4 are not energized because they are open or OFF. The primary side voltage is inverted with the negative flow direction forwarded to the secondary side of the transformer and diodes D2 and D3 will flow current to the filter circuit and the output side.

Figure 4b is the same as condition 2. When the converter is in condition 4 there is a second deadtime process with the four switching components in the open or OFF condition so that the output current flows to the four diodes [11].

The value of the output voltage on the Full Bridge Converter (V_{out}) is obtained from the time integral result of the inductor voltage (V_L) during the switching period T, shown in equation 15.

$$V_{out} = 2 \times \frac{1}{T}\int_0^{dT}\left(\frac{N_s}{N_p} V_{in} - V_{out}\right) dt + \int_{T/2}^{T/2+dT} - V_{out}\, dt \tag{15}$$

Thus, we get Equation 16.

$$V_{out} = 2\frac{N_s}{N_p} V_{in} d \tag{16}$$

The output of the Full Bridge Converter is obtained from the output power (Pout), with the value according to equation 17.

$$P_{out} = \eta P_{in} = \eta V_{in} I_{primary(avg)} d \quad (17)$$

The average primary current ($I_{primary(avg)}$) can be calculated from equation 18.

$$I_{primer(avg)} = \frac{P_{out}}{\eta V_{in} d} \quad (18)$$

Figure 5 shows the shape of each wave that flows in the converter type topology Full Bridge Converter, namely VQ1; Q4, VQ2, Q3, V_P, I_{peak}, V_s, and I_L. In the switching process, during condition 1, Q1 and Q4 are in the ON condition or the switch is closed, while Q2 and Q3 are in the OFF state or the switch is open. Condition 2 is when all switches are OFF. In condition 3 the opposite condition applies to condition 1, namely switches Q2 and Q3 are in the ON state or the switch is closed while Q1 and Q4 are in the OFF state or the switch is open. Condition 4 is the same as condition 2 when all switches are OFF.

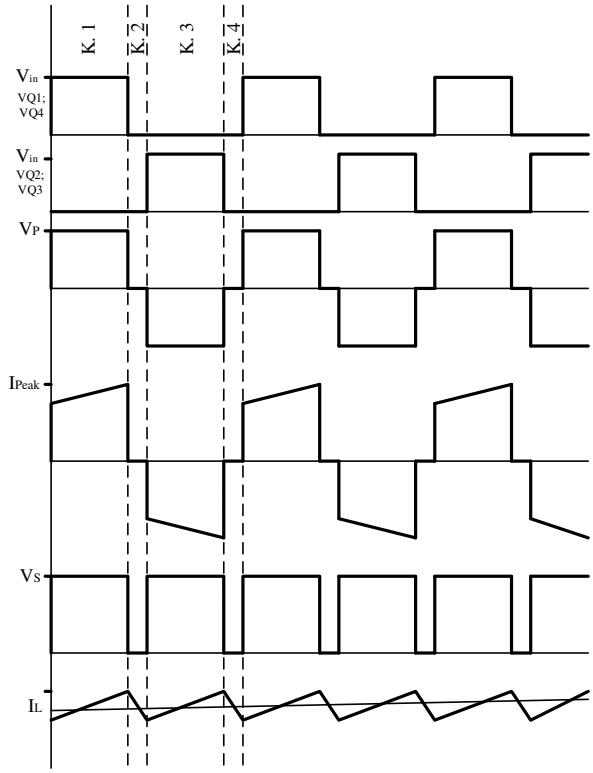

Fig. 5. Figure each parameter value of the full bridge converter wave [10].

The picture also shows the waves resulting from the switching process of primary voltage (V_P) and primary current (I_{Peak}) which form a square wave on the positive and negative sides according to the direction of current flowing in the converter. The secondary voltage (V_S) is the voltage on the secondary side of the transformer in the form of a wave after being rectified by a full bridge rectifier, and the Inductor Current (I_L) is the current flowing in the LC filter to reduce current and voltage losses at the converter output [10].

TABLE II. CONVERTER PARAMETER SYSTEM

Parameter	Value
V_{in}	35.6 V
f_s	100 kHz
N_1:N_2	1:10
L	1.29 mH
C	1.33 uF

Table 2 shows the parameter values used in the system as a DC-DC power converter. In accordance with the system design, the converter is used to increase the DC voltage rating with a ratio value of 1:10.

C. Fuzzy Type-2 Methods

Fuzzy Type-2 in this system is designed based on the theory of fuzzy logic. Considering the advantages of Fuzzy Type-2 over Fuzzy Type-1, namely in terms of noise reduction, transient state, and based on uncertainty settings. Three-dimensional form of Membership Function as a characteristic of Fuzzy Type-2 Sets, provides degrees of freedom to track and resolve any difficulties in finding the right membership function [12]. It is based on that fuzzy has adaptive properties so that it will increase the accuracy of the system from unknown parameters. Therefore, it takes a challenge to design the fuzzy on the system in order to produce the maximum value of the output power of the solar panel.

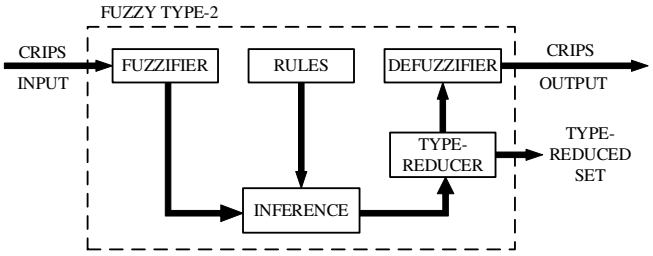

Fig. 6. Structure of fuzzy type-2 [13].

Fuzzy Type-2 design on the MPPT system is used to obtain the output parameter value of the fuzzy set, namely the duty cycle for the switching elements on the Full Bridge Converter. The system of the Fuzzy Type-2 set shown in Figure 6 consists of input crips which will be processed into a Fuzzy Type-2 membership function by the fuzzifier, and processed on the interference engine based on the structure of the rule base. Due to the computation on the interference engine using the Type-2 interval, it will be reduced to the Type-1 interval by the Type-reducer. Defuzzification will convert into crips output so that it can produce a duty cycle value. For Fuzzy Type-2 which is used in the system is the Fuzzy Sugeno type.

The MPPT method uses Fuzzy Type-2, the input parameters in this system are Error and ΔError is shown in equation 19 and equation 20.

$$E(k) = \frac{P(k) - P(k-1)}{V(k) - V(k-1)} = \frac{\Delta P}{\Delta V} \quad (19)$$

$$\Delta E(k) = E(k) - E(k-1) \quad (20)$$

Equations 19 and 20 are shown where E(k) and ΔE(k) are the error and the change in error at the sampling time (k). P(k) and V(k) are the power and output voltage from the Solar Panel.

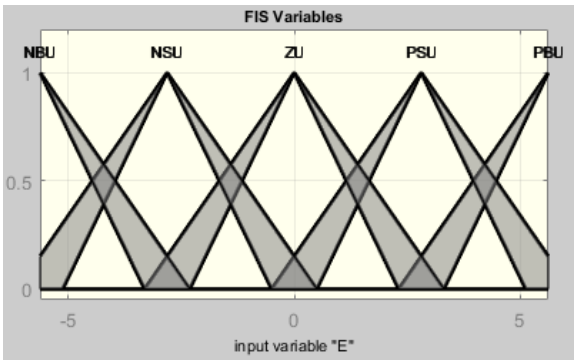

(a)

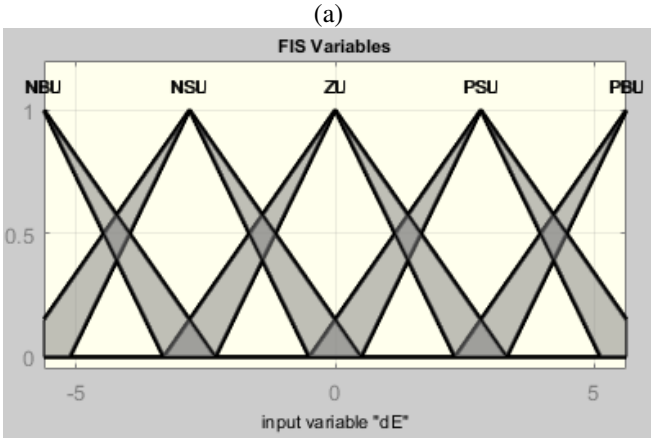

(b)

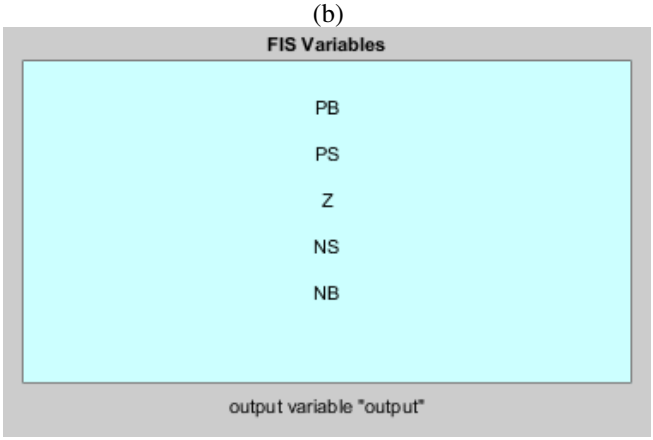

(c)

Fig. 7. Membership function fuzzy type-2 on the system (a) MF error (b) MF Δerror (c) MF output.

In the inference engine, data processing is conducted based on input values from Membership Function Fuzzy Type 2, Error and ΔError according to Figure 7.

TABLE III. FUZZY TYPE-2 RULE BASE

Δu(k)		***ΔE(k)***				
		NB	NS	ZE	PS	PB
E(k)	NB	PB	PS	NB	NB	NB
	NS	ZE	ZE	NS	NS	NS
	ZE	NS	ZE	ZE	ZE	PS
	PS	PS	PS	PS	ZE	ZE
	PB	PB	PB	PB	NS	NS

Membership Function values in Fuzzy Type 2 have a 3-dimensional structure at each point in a 2-dimensional area called Footprint of Uncertainty (FOU). In the FOU field there are 2 upper and lower boundaries, namely Upper MF and Lower MF.

Based on the five different fuzzy levels, input parameters are used with the names NB (Negative Big), NS (Negative Small), ZE (Zero), PS (Positive Small), and PB (Positive Big). According to Table 3, the Fuzzy Type-2 system is governed by 25 different rules [14].

In accordance with the Fuzzy Type 2 structure, the output from the interference engine will be treated at Type-Reduction. There are various types of type-reduction methods including center of sets, centroid, height and modified height. The output interval value is determined from each of the left and right points, the value of u_r and u_l, as well as the number of rules that have been previously arranged. Karnik-Mendel proposed an iteration procedure to obtain u_r and u_l values. Because there is an interval in the Type-Reducer sets value, the defuzzification output value in the form of crips is obtained through the average value of the leftmost point (u_l) and the rightmost point (u_r) [15] in the form of the equation 21.

$$u_{ft2}(e) = \frac{u_r + u_l}{2} \quad (21)$$

III. SIMULATION RESULT AND DISCUSSION

In this paper, research is carried out by making models and system simulations made using MATLAB/Simulink software with the parameters that have been set in the materials and methods chapter.

The model made in the form of a simulation block diagram on a solar panel system with input variables of irradiation and temperature, is connected to the converter circuit and the MPPT method used. Figure 8 shows the modeled block diagram simulation. Figure 9 is a MPPT block diagram using Fuzzy type-2 with Sugeno type and the output is a crips duty cycle value which is compared with a triangular wave at a frequency of 100 kHz to produce a signal Pulse Width Modulation (PWM) as the driver of the power converter.

The solar panels used are two static solar panels each 100 WP arranged in series with the input parameters in the form of irradiation and temperature values. The irradiation value and temperature in this study were set at low, medium, and high conditions by considering the reliability and accuracy test of the MPPT method on the input variables used. There are two test models as research, namely using model 1 with the input variable set in the irradiation range of 300 W/m2 to 1000 W/m2 with a fixed temperature. In Model 2 the input variable is set to an irradiation range of 300 W/m2 to 1000 W/m2 and a temperature range of 25°C to 55°C.

The percentage of power accuracy will be searched for each MPPT method and the results will be compared. Power accuracy is the value of the test results using the MPPT method compared to the ideal power contained in the PV for each irradiation. Power accuracy is indicated by the percentage accuracy (Acc) result. can be seen in the formula in the equation 22.

$$Acc(\%) = \left(1 - \frac{P_{PVideal} - P_{PVmethod}}{P_{PVideal}}\right) \times 100\% \quad (22)$$

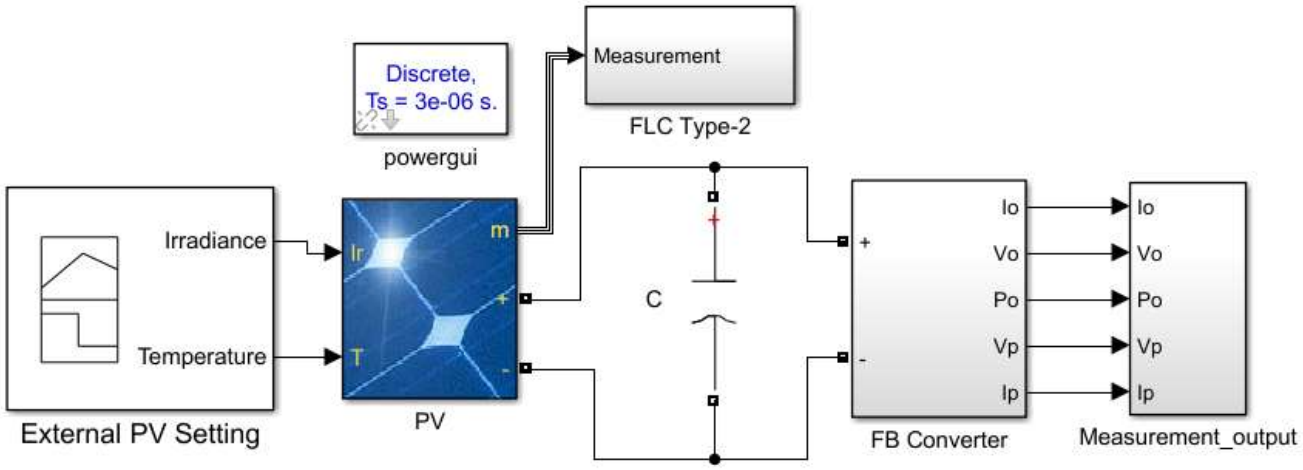

Fig. 8. Modeling the overall system.

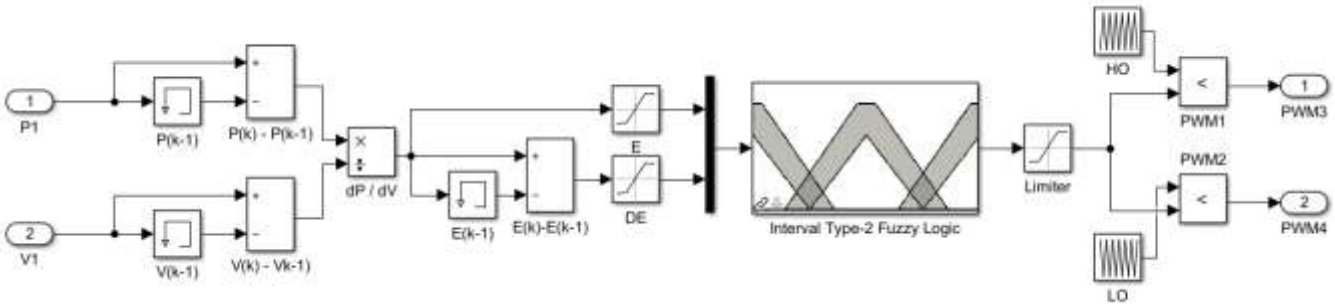

Fig. 9. MPPT fuzzy type-2 block diagram model.

The Maximum Power Point Tracking method used is to compare the simulation results between Fuzzy Type-1 and Fuzzy Type-2. From this comparison, it is obtained the value of the output power from the solar panel to reach its maximum point when set using both methods as well as the average power accuracy value.

The first test is in accordance with Figure 10 in model 1, which provides an input variable set at 300 W/m2 to 1000 W/m2 irradiation with a fixed temperature at 25°C. The results of model 1 test data can be seen in Table 4.

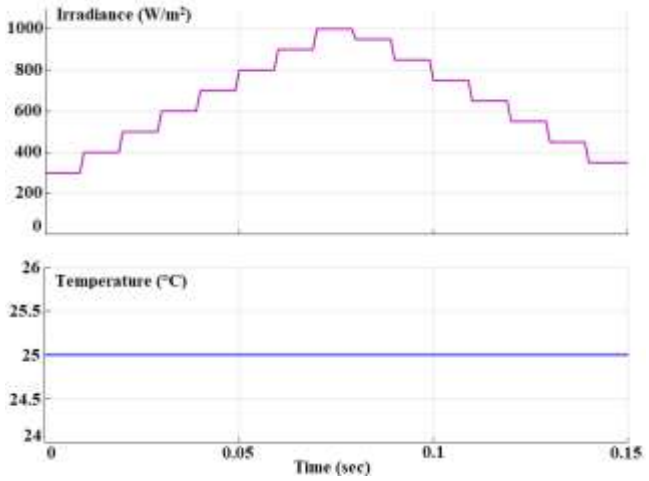

Fig. 10. Input variables irradiation and temperature model 1.

The test results on model 1 show that the minimum irradiation is 300 W/m2 with the result of the output power using Fuzzy Type-2 of 37.62 Watt with an ideal output power of 59.28 Watt. Then the percentage of power accuracy at minimum conditions is 63.46%.

In medium irradiation, which is 650 W/m2, the output power using Fuzzy Type-2 is 129.8 Watt with an ideal output power of 130.4 Watt. From the medium irradiation data, the percentage of power accuracy is 99.53%. At the maximum irradiation is 1000 W/m2 with the output power using Fuzzy Type-2 is 180.8 Watt with the ideal output power is 200.1 Watt. Obtained the percentage of power accuracy at the maximum irradiation is 90.35%.

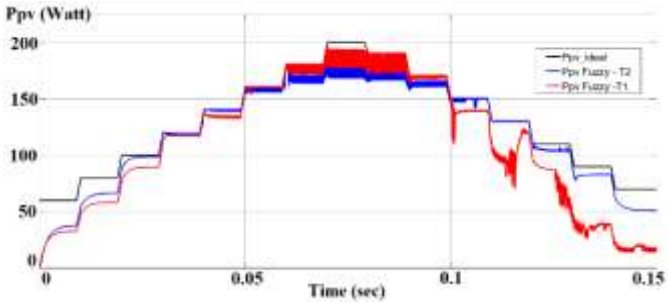

Fig. 11. Solar panel output power (P_{PV}) on variable input model 1.

This shows that the input variable Solar Panel Model 1 at a low and medium irradiation level, the accuracy value of the output power using Fuzzy Type-2 is faster in response and also in a stable state. At the maximum irradiation level.

Fuzzy Type 2 can reduce the ripple and transient values of the output power, as well as when the irradiation conditions decrease as shown in Figure 11, the output power of the Solar Panel using Fuzzy Type-2 continues to work steadily reaching the MPP point than Fuzzy Type-1.

TABLE IV. SIMULATION RESULTS DATA ON THE INPUT VARIABLE MODEL 1

Irr (W/m²)	Temp (°C)	P_{PV} (W)	Type-1		Type-2	
			P_{PVT1} (W)	Acc (%)	P_{PVT2} (W)	Acc (%)
1000	25	200.1	187.9	93.9	180.8	90.3
950		190.2	175.2	92.1	170.1	89.4
900		180.3	173.1	96.0	166.5	92.3
850		170.4	168.2	98.7	162.4	95.3
800		160.5	158.6	98.8	156.5	97.5
750		150.5	138.2	91.8	148.7	98.8
700		140.5	134.3	95.5	139.9	99.5
650		130.4	98.77	75.7	129.8	99.5
600		120.3	119.8	99.5	118.2	98.2
550		110.2	89.17	80.9	105.2	95.4
500		100	89.47	89.4	98.58	98.5
450		89.84	38.48	42.8	82.83	92.1
400		79.66	58.10	72.9	66.53	83.5
350		69.47	18.00	25.9	53.33	76.7
300		59.28	32.83	55.3	37.62	63.4

The second test is in accordance with Figure 12 in Model 2, which provides an input variable set at an irradiation level of 300 W/m² to 1000 W/m² with a temperature set at 25°C to 55°C. The results of model 2 test data can be seen in Table 5.

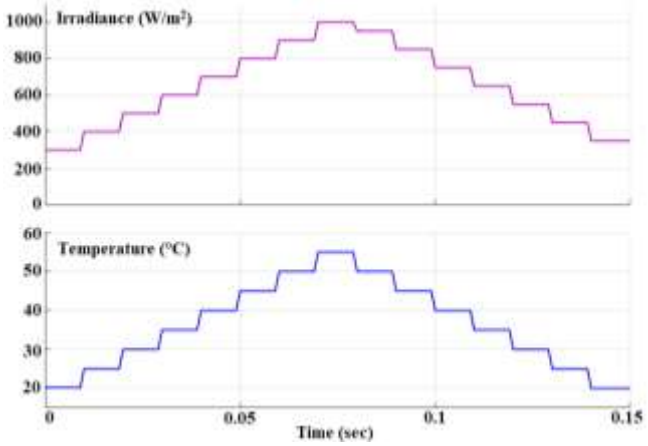

Fig. 12. Input variables irradiation and temperature model 2.

In model 2 the condition of the output power of the solar panel when the temperature changes has a lower value, compared to model 1 because in model 1 the temperature value is in the Solar Panel test condition, which is 25°C with irradiation of 1000 W/m², so that the maximum output according to the datasheet is 200.1 Watt.

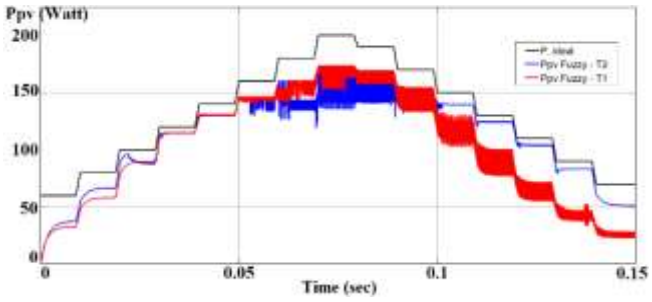

Fig. 13. Solar panel output power (P_{PV}) on variable input model 2.

The test results were obtained under irradiation conditions and a minimum temperature of 300 W/m²; 25°C, the result is that the output power using Fuzzy Type-2 is 37.30 Watt with the ideal output power of a Solar Panel is 59.28 Watt. The percentage of power accuracy at minimum conditions is 62.92%. In irradiation conditions and medium temperature 650 W/m²; 35°C, the result is that the output power using Fuzzy type-2 is 124.7 Watt with the ideal output power is 130.4 Watt. The percentage of power accuracy in intermediate conditions is 95.62%. For irradiation conditions and a maximum temperature of 1000 W/m²; 55°C, the output power obtained using Fuzzy Type-2 is 173.6 Watt with the ideal output power of a Solar Panel is 200.1 Watt. The percentage of power accuracy at maximum conditions is 86.85%.

TABLE V. SIMULATION RESULT DATA ON THE INPUT VARIABLE MODEL 2

Irr (W/m²)	Temp (°C)	P_{PV} (W)	Type-1		Type-2	
			P_{PVT1} (W)	Acc (%)	P_{PVT2} (W)	Acc (%)
1000	55	200.1	173.7	86.8	173.6	86.8
950	50	190.2	169.5	89.1	169.4	89.0
900	50	180.3	159.2	88.2	143.8	79.7
850	45	170.4	154.6	90.7	142.8	83.8
800	45	160.5	145.4	90.5	145.4	90.5
750	40	150.5	126.1	83.7	139.5	92.6
700	40	140.5	130.2	92.6	130.8	93.0
650	35	130.4	97.59	74.8	124.7	95.6
600	35	120.3	115.2	95.7	114.9	95.5
550	30	110.2	71.82	65.1	103.8	94.1
500	30	100	89.71	89.7	96.00	96.0
450	25	89.84	47.18	52.5	83.19	92.5
400	25	79.66	58.21	73.0	66.48	83.4
350	20	69.47	28.62	41.1	54.44	78.3
300	20	59.28	32.50	54.8	37.30	62.9

If it is seen in Figure 13 that the Fuzzy Type-2 in the minimum condition increases to the maximum, until it drops back to the minimum, it shows that the tracking stability reaches its MPP compared to Fuzzy Type-1 which is less stable and has a large range of ripple and noise.

After obtaining the data from the parameters in Models 1 and 2, the results of the average percentage of the output power accuracy are analyzed using the MPPT method with two different algorithms, which are compared between Fuzzy Type-2 and Fuzzy Type-1.

TABLE VI. PERCENTAGE OF POWER ACCURACY ON 2 MODELS

Irradiation & Temperature	Rate Percentage (%)	
	Fuzzy Type-1	Fuzzy Type-2
Model 1	80.64	91.40
Model 2	77.93	87.63

The Fuzzy Type-2 method has a Membership Function form with a three-dimensional structure at each point with an upper and lower position resulting in tracking the uncertainty of the error and Δerror value is wider and the resulting ripple is lower, so that in Table 6 the percentage value average accuracy of the output power is shown. Using the Fuzzy Type-2 Algorithm is more accurate than Fuzzy Type-1.

IV. CONCLUSION

In this paper, based on testing using Model 1 with fixed irradiation and temperature input variables, and Model 2 with input variables for changes in irradiation and temperature by comparing the MPPT method with Fuzzy Type-1 and Fuzzy Type-2 algorithms, The results average percentage accuracy the output power of Solar Panel in Model 1 using Fuzzy Type-1 is 80.64% while Fuzzy Type-2 is 91.40%. The average percentage accuracy of output power Solar Panel in Model 2 with Fuzzy Type-1 is 77.93%, while Fuzzy Type-2 is 87.63%. Fuzzy Type-2 has a power tracking value closer to the MPP value at low, medium, to high levels of irradiation parameters, and is more stable to ripples and transients during conditions of decreasing irradiation.

REFERENCES

[1] K. Anoune, M. Bouya, M. Ghazouani, A. Astito, and A. B. Abdellah, "Hybrid renewable energy system to maximize the electrical power production," in 2016 International Renewable and Sustainable Energy Conference (IRSEC), Marrakech, Nov. 2016, pp. 533–539. doi: 10.1109/IRSEC.2016.7983992.

[2] A. K. Abdelsalam, A. M. Massoud, S. Ahmed, and P. N. Enjeti, "High-Performance Adaptive Perturb and Observe MPPT Technique for Photovoltaic-Based Microgrids," IEEE Trans. Power Electron., vol. 26, no. 4, pp. 1010–1021, Apr. 2011, doi: 10.1109/TPEL.2011.2106221.

[3] Z. Ons, J. Aymen, A. Craciunescu, and M. Popescu, "Comparison of Hill-Climbing and Artificial Neural Network Maximum Power Point Tracking Techniques for Photovoltaic Modules," in 2015 Second International Conference on Mathematics and Computers in Sciences and in Industry (MCSI), Sliema, Malta, Aug. 2015, pp. 19–23. doi: 10.1109/MCSI.2015.24

[4] Zhanghong, Lishengzhu, Zhangxiaonan, and Xiayilan, "MPPT control strategy for photovoltaic cells based on fuzzy control," in 2016 12th International Conference on Natural Computation, Fuzzy Systems and Knowledge Discovery (ICNC-FSKD), Changsha, China, Aug. 2016, pp. 450–454. doi: 10.1109/FSKD.2016.7603215.

[5] B. Subudhi and R. Pradhan, "A Comparative Study on Maximum Power Point Tracking Techniques for Photovoltaic Power Systems," IEEE Trans. Sustain. Energy, vol. 4, no. 1, pp. 89–98, Jan. 2013, doi: 10.1109/TSTE.2012.2202294.

[6] D. Wu, "On the Fundamental Differences Between Interval Type-2 and Type-1 Fuzzy Logic Controllers," IEEE Trans. Fuzzy Syst., vol. 20, no. 5, pp. 832–848, Oct. 2012, doi: 10.1109/TFUZZ.2012.2186818.

[7] S. Soltani, N. Square, and M. J. Kouhanjani, "Fuzzy Logic Type-2 Controller Design for MPPT in," p. 7, 2017.

[8] S. B. Chavan and M. S. Chavan, "Design and implementation of full bridge DC-DC converter for photovoltaic application," in 2015 International Conference on Energy Systems and Applications, Pune, India, Oct. 2015, pp. 466–469. doi: 10.1109/ICESA.2015.7503393.

[9] O. Ibrahim, N. Z. Yahaya, N. Saad, and K. Y. Ahmed, "Development of Observer State Output Feedback for Phase-Shifted Full Bridge DC–DC Converter Control," IEEE Access, vol. 5, pp. 18143–18154, 2017, doi: 10.1109/ACCESS.2017.2745417.

[10] M. H. Rashid, Power electronics: devices, circuits, and applications, Fourth edition. Upper Saddle River, NJ: Pearson, 2014.

[11] J. van Rensburg, "Full Bridge DC-DC converter as input stage for fuel cell based inverter system," p. 5.

[12] A. T. Azar, "Overview of Type-2 Fuzzy Logic Systems:," International Journal of Fuzzy System Applications, vol. 2, no. 4, pp. 1–28, Oct. 2012, doi: 10.4018/ijfsa.2012100101.

[13] J. M. Mendel, R. I. John, and F. Liu, "Interval Type-2 Fuzzy Logic Systems Made Simple," IEEE Trans. Fuzzy Syst., vol. 14, no. 6, pp. 808–821, Dec. 2006, doi: 10.1109/TFUZZ.2006.879986.

[14] N. Hussein Selman, "Comparison Between Perturb & Observe, Incremental Conductance and Fuzzy Logic MPPT Techniques at Different Weather Conditions," IJIRSET, vol. 5, no. 7, pp. 12556–12569, Jul. 2016, doi: 10.15680/IJIRSET.2016.0507069.

[15] N. Altin, "Single phase grid interactive PV system with MPPT capability based on type-2 fuzzy logic systems," in 2012 International Conference on Renewable Energy Research and Applications (ICRERA), Nagasaki, Japan, Nov. 2012, pp. 1–6. doi: 10.1109/ICRERA.2012.6477335.